



EFFECT OF CHROMIUM SUBSTITUTION ON STRUCTURAL, ELECTRICAL AND MAGNETIC PROPERTIES OF NANOCRYSTALLINE SUBSTITUTED STRONTIUM HEXAFERRITES

**Sheela A. Pawade¹, S. R. Gawali², P. R. Moharkar³, Vivek M. Nanoti⁴ and
Kishor G. Rewatkar⁵**

1 Dept. of Applied Physics, Rajiv Gandhi College of Engineering, Chandrapur

2 Department of Physics, Ambedkar College, Chandrapur.

3 Department of Physics, A.C.S. College, Chandrapur

4 Department of Applied Physics, Priyadarshini College of Engineering, Nagpur

5 Department of Physics, Dr. Ambedkar College, Nagpur

Corresponding author Email : pmoharkar103@gmail.com

Abstract:

Strontium M-Type hexaferrite have been of considerable interest for many years due to their appropriate magnetic properties which applied in many applications such as microwave devices, high density magnetic recording, electronic devices and medicine. Several cations such as Cr³⁺, Al³⁺, In³⁺ and etc substituted in order to improve the magnetic and electrical properties of strontiumhexaferrite. Nanosize Chromium substituted strontium hexaferrite SrCr_xFe_{12-x}O₁₉ (x=0-8) synthesized by microwave assisted Solgel auto-combustion route using urea as a fuel/reductant and nitrates as oxidants. The structural and magnetic behaviour of these samples were studied using X-ray diffraction (XRD), vibrating sample magnetometer and Transmission Electron Microscope (TEM). (XRD) studies reveal that microwave-assisted combustion synthesis route yields materials with higher degree of compositional stability and phase purity. Both a and c lattice parameters calculated systematically decrease with increasing Cr content. The effects of Cr³⁺ ions on the Strontium Lanthanum ferrites were reported and discussed in detail. The site preference of Cr³⁺ and magnetic properties of the ferrites have been studied using hysteresis. The results show that the magnetic properties are closely related to the distributions of Cr³⁺ ions on the five crystallographic sites. The saturation magnetization systematically decreases, however, the coercivity decreases with Cr concentration. The magnetization results indicate that the Cr³⁺ ions preferentially occupy the 2a, 12k, and 4fVI sites.

Keywords:

Strontium ferrite, X-ray density, porosity, magnetization, coercivity, retentivity etc.





Introduction:

Strontium hexaferrite ($\text{SrFe}_{12}\text{O}_{19}$) ($M = \text{Ba, Sr, Pb}$) [1] which crystallizes in the hexagonal system and has a uniaxial magnetoplumbite structure, (space group $P6_3/mmc$) displays distinctive magnetic characteristics, good chemical stability, good tribological properties and a weak temperature dependent coercivity at about room temperature. Alabanese et al. [2] showed that in cationic substituted M-type hexagonal ferrites the distribution of metallic ions among the different sub lattices is greatly modified by replacement of Ba with Sr. The permanent magnetic properties of hard ferrites are known to depend on their microstructural characteristics such as grain size, porosity, the presence of second phases and growth anisotropy [3]. High remanence requires a high sintered density and growth anisotropy, whereas high coercivity requires a small grain size [4]. Since the discovery of M-type hexagonal ferrites, extensive research has been carried out to improve their magnetic properties, particularly by the use of cationic substitutions [5, 6]. Some workers have substituted light rare-earth ions (LRE) such as La, Pr and other metal cations for Sr (Ba) and Fe respectively, taking into account of the ionic radius of elements [7]. The properties of ferrites are strongly influenced by composition and synthesis method. The rare earth substitution was employed to inhibit the grains growth [8] and to promote ferritization reaction [9]. The lanthanides also improve the mechanical materials hardness [10]. The experiments carried out by Dung [11] showed that the La substitutions improve hard magnetic properties. The saturation magnetization and other properties are closely related to the distribution of the doping ions on five Fe crystallographic sites. In 1995 Wartewig [12] first investigated Cr distribution in Cr-doped Sr-M ferrites prepared by a solid state reaction. Mössbauer spectra of chromium-doped strontium ferrites found that the Cr^{3+} ions initially substituted Fe at 2a octahedral site and followed the preference on 12k and 4fVI octahedral sites, respectively, due to the crystal field effect. The Sr-M hexaferrite structure is symbolically assigned as RSR^*S^* where R is a rhombohedral block forming a





three-layer block (two O4 layers and one SrO3 layer) with composition as $Sr_{2+Fe_6}O_{12}$ and S is a spinel block forming a two O4 layer block with composition as Fe_6O_8 . The blocks signified by asterisk have been rotated by 180° about the c-axis. The Sr-M structure consists of five distinct Fe crystallographic sites, i.e., three octahedral (12k, 4fVI and 2a) sites, one tetrahedral (4fIV) and one trigonalbipyramid (2b) site [13]. In the present investigation we have synthesized M type nano sized Cr⁺³ doped Srhexaferrites by applying microwave assisted Sol-gel auto combustion process and we systematically amount on properties Viz crystal structure, electrical conduct(Hc) and retentivity (Mr) properties of Srhexaferrites. Conventional solid state method, as the classical ceramic route for preparing strontiumhexaferrite, requires a high calcining temperature (1200-1300°C) which induces sintering and aggregation of particles. Furthermore, the milling process to reduce the particle size from multi domain to single domain, generally yields non-homogeneous mixture on a microscopic scale and results in lattice strain in the materials [14]. Recently, the sol-gel auto-combustion (citrate-nitrate), as a novel process, based on the gelling and subsequent combustion of an aqueous solution containing salts of the desired metals and some organic fuels, has been given a voluminous and fluffy product with large surface area [15].

Material and Method:

y = 1 were synthesized using a sol-gel auto combustion process. All chemicals used for this synthesis were of analytical reagent grade. The experimental sequence may be summarized as follows: A yellow-brown transparent aqueous solution of $Sr(NO_3)_2$, $Fe(NO_3)_3 \cdot 9H_2O$, $Cr(NO_3)_3 \cdot 9H_2O$, $La(NO_3)_3 \cdot 6H_2O$, $CO(NH_2)_2$ was prepared. The solution was heated under constant stirring at a temperature of about 140 °C in a Pyrex beaker so that it concentrated slowly without producing any precipitation, but changed its viscosity and color, until it turned into a brown gel. When the temperature of the microwave oven was raised to about 250–300 °C, the gel swelled into foam and underwent a self-





propagating combustion reaction changing the brown gel into black powders. The entire combustion process was over after half an hour. The resulting black ashes were ground in an agate mortar, put into alumina crucibles, and then calcined at 800°C for 1h until complete decomposition of the carbonaceous residues and solid state ionic saturation magnetization (Ms), Coercivity reaction occurred. Calcined powders were ground and after adding polyvinyl alcohol as a binder mixtures were shaped into pellets using hydraulic press under uniaxial pressure of 75kNm⁻². These pellets of each composition were then sintered at 1200°C in electric furnace for 7-8 hours. During sintering process crystallization gave rise to a hexagonal polycrystalline phase. Fig.1 shows modified version of domestic microwave oven used in the present work having 2.45 GHz frequency.

Experimental details : Powders of Sr_{1-x}La_xFe₁₂O₁₉ with (0

Result and Discussion:

Hexaferrite SrFe₁₂O₁₉ was first prepared by Adelskold in 1983 [16]. He also determined the crystal structure of this compound to be iso-structural with magnetoplumbite (M) with space group P6₃/mmc. Lattice constant „a” shows less variation and lattice constant „c” initially varies rapidly followed by slow variation with substitution. This is in agreement with the fact that all hexagonal ferrites exhibit constant lattice parameter „a” and variable parameter „c” by Deschamp [17], which shows that „c” is more susceptible to stoichiometric changes than „a” [18]. Fig 2 shows XRD pattern of high purity Cr doped strontium ferrites with different doping concentrations. All peaks belong to M-structure ferrite phase and no intermediate phases are observed. The lattice parameter „a” and „c” are in the range of 5.5 to 6 Å and 22.15 to 23.55 Å pertaining to SG: P6₃/mmc (no. 194). The substitution does not affect much on the crystal symmetry (table- 2) This is due to relatively small ionic radii of Cr³⁺ (0.64Å) (comparing with that of Fe (0.67Å) for sixfold co-ordination. As a result the cell volume of the compounds decreases after being doped. There are two





formula units in a unit cell. There are ten layers of Oxygen atoms along the c-axis. The structure built up from small units: a cubic block (S) having the spinel type structure and a hexagonal (R) block containing Sr^{+2} ions. The iron atoms are positioned at five crystallographically different sites as shown in table-1. The variation in the values of resistivity and hence conductivity and activation energies may be concluded that an electron hopping mechanism between Fe^{3+} ions might reasonably be assumed and so the conductivity is related to the presence of Fe^{2+} ions in sample. The decrease in activation energy with increase in x may be due to several reasons such as small number of Fe^{2+} are generally formed during sintering process which increase the conductivity due to increased hopping between Fe^{2+} and Fe^{3+} by Mitrar. The conductivity is found to be almost linearly decreasing with reciprocal of temperature [19]. Figure 3. s 52 nm) (Fig. 4). The effect of Cr^{+3} ions on the saturation magnetization, retentivity and coercivity of compounds under study are shown in Fig. 5. The increase of Cr^{+3} ions content, the saturation magnetizations deduced from law of approach to saturation show the decrease in coercivities. The magnetizations are closely related to distribution of Cr^{+3} ions on each crystallographic sites and then magnetic dilution or non-collinear structure (spin canting) with the substitution of Fe^{+3} ions by lower magnetic movement ions, in this case Cr^{+3} ions. It is evident that the areas on octahedral 12k and 4fVI sites tend to decrease with the doping content. In other words this means that the Cr^{+3} ions could be entering into the octahedral 12k and 4fVI sites. From magnetic results, it should be noted that Cr^{3+} ions preferentially occupy on octahedral 12k, 2a and 4fVI sites resulting in the dramatic drop in saturation magnetization and the lowering of the Curie temperature. The Fe^{3+} -O- Fe^{3+} super exchange interaction would be partially disrupted by substituting Fe^{3+} with Cr^{3+} on 12k site. Furthermore, it is known that for each 4fIV site, there are three neighboring 12k sites and the preference of Cr^{3+} ions on 12k site strongly perturbs the 12k-4fIV magnetic super exchange interaction. The site occupancies as determined by Mössbauer spectra





show that the lanthanum innig effect between the interstitial sites. The constriction may be regarded as disproof of the shape effect [21, 22] originated anisotropy of Sr-ferrites. Further investigations like crystal and domain structure under low temperature should be taken in consideration and a new mechanism rather than thermal fluctuations and thickness-variety of Bloch Wall for high and low temperature [23] needs to be established In case of samples SrLaCr₆Fe₅O₁₉ and SrLaCr₈Fe₃O₁₉ the noisy regions in hysteresis are observed. The starting magnetization for these compounds exhibit comparably large amplitude oscillations at the vibrating frequency $f/2$, the phases of which are very different. However, after attainment of saturation these larger amplitude vibrations gets suppressed to large extend and are replaced by small amplitude vibrations at frequency „ f “. We note that in the first oscillation are present on both side of the central, post and pre saturation hysteresis loop, show additional small amplitude, higher frequency oscillations, which may be higher harmonics of „ f “. This occurrence may be due to randomness of the oscillation phases, The figure demonstrates that steps in the magnetization do not necessarily have unusual hysteresis effect $\approx 8, y = 1$) under high magnetic field (15 KOe) Absolutely there is no constriction in SrLaFe₁₁O₁₉. Absence of constriction in SrLaFe₁₁O₁₉ may imply existence of a certain contact between constricted loops and the ionic contents of both Cr and Fe elements. While the reason for no constriction in CrLaFe₁₁O₁₉ could not be explained using Jida"s results since there is no clue of the influences of cation ratio on directional ordering in this theory [20]. We therefore assumed that the exchange interaction between Cr⁺³ and Fe⁺³ and ions within a certain distance on the interstitial side may play a crucial role in this phenomenon. In addition we have investigated the effect of aging time on the influence the interaction between cations/anions and hence repressed the constriction. contribution from the large single ion anisotropy from rare earth sublattice. Similar results are reported [21] in case of partial substitution of Fe⁺³ by Tb⁺³ and Dy⁺³ ions in cobalt ferrite system. Substitution of rare earth ion into the





spinel structure has been reported to lead to structural distortion [22] and to induce strains in the materials and significantly modify the magnetic and electric behavior. The particle morphology was examined by Transmission Electron Microscope (TEM). The particle size was in nano scale ($\leq x \leq$ shows the hysteresis loops of $\text{SrLa}_x\text{Fe}_{12-x-y}\text{Cr}_y\text{O}_{19}$ with (0

Conclusion:

The variation in the values of resistivity and hence conductivity and activation energies may be concluded that an electron hopping mechanism between Fe^{3+} ions might reasonably be assumed and so the conductivity is related to the presence of Fe^{2+} ions in sample. The partial substitution of rare earth La^{3+} ions for Fe^{3+} had enhanced the total coercive field by almost 30%. The saturation magnetizations are closely related to the distribution and concentration of Cr^{3+} ions on the five crystallographic sites. Magnetic results revealed that Cr^{3+} ions preferentially occupy the octahedral 2a, 4f₂, and 12k sites. With Cr^{3+} entering the Fe^{3+} crystallographic sites, the saturation magnetization dramatically falls and coercivity also shows decreasing trend. The decrease in magnetization is therefore attributed to Cr^{3+} ions occupying on the spin up Fe sites. (2a and 12k sites) and magnetic dilution or on-collinear structure. It is evident that the $\text{Fe}^{3+}-\text{O}-\text{Fe}^{3+}$ super exchange interaction may be weakened by Cr^{3+} ($3d^3$) substituting into some Fe ($3d^5$) sites. ~All the synthesized compounds show magnetoplumbite (M) structure with single phase. The grain size of the samples is in the range of nano size (

References:

Lirington J.D, Jox, 42, (1990)

Albanese G, Carbuicchio M. , Deriu A. , Nuovo Cimento B15,147(1973)

Singh A., Narang B. , Singh K., Pandey O.P. , Kotnala R.K. , Ceram. J. Proc. Res. 11,241 (2010)





- Besebicar S., Drfenik M., Mag. J. Magn. Mater. 101, 307 (1991)
- Wohlfarth E.P., Handbook of Magnetic Material (North-Holland, Amsterdam, (1982)
- Cullity B.D., Introduction to Magnetic Materials (Addison-Wesley, Massachusetts, 1972)
- Liu X, Zhong W., Yang S., Yu Z., Gu B., Phys. Stat. Sol. 193,
- Qiu J., Gu M. and Shen H. (2005) J. Magn. Magn. Mater. 295, 263,
- Taguchi H. (1997) J. Phys. IV France 7, C1-299.
- Troczynski T.B. and Nicholson P.S. (1989) J. Am. Ceram. Soc. 72, 1488.
- Dung N.K., Minh D.I., Cong B.T., Chau N. and Phue N.X. (1997) J. Phys. IV France, C1-313.
- Wartewig P, Melzer K, Krause M, Tellgren R, 1995 J. Magn. Magn. Mater. 140-144 2101.
- Kojima H, in: Wohlfarth E.P. (Ed.), 1982 Ferromagnetic Materials: Handbook on the Properties of Magnetically Ordered Substances, North-Holland, Amsterdam, , p. 305
- Kingery, W. D. et al. (1976). Introduction to Ceramic, John Wiley and Sons Inc.
- Mali, A., & Ataie, A. (2004). Ceramic International., 30, 1979-1983.
- Adelskold V, Arkiv Kami Min Geol, 1983 A 12, 1-9
- Deschamp A., Bortant E., C. R. Acad. Sci. Paris, 224, 3069, (1957).
- Dorofte C.I., Rezlescu E., Popa P., J. of optoelectronics and Advance Mater., 8, 1023-1027, (2006).
- Mitra R., Puri R., and R Mandiratfa R., J. Mater Sci, 27, 1275, (1992). Jida S, Sekizawa H, Aiyama Y, 1955 J. Phy. Soc. Jpn. 10 907





Cheng F, Liao C, Kuang J, Xu Z, Yan C, Chen L, Zhao H, Liu Z 1999 J. Appl. Phy.85 2782

Rezlescu N, Rezlescu E 1994 J. Phys: Condens Matter 6 5707

Dong H C, Lee W, Shim In-Bo, Kim C S 2006 J. Magn. Magn. Mater. 304 243

Table 1. Crystallographic sites of Fe ions.

Sub lattice	Co-ordination	Number of ions	Spins
12K	Octahedral	6	Up
4f ₁	Tetrahedral	2	Down
4f ₂	Octahedral	2	Down
2a	Octahedral	1	Up
2b	Trigonal bi- pyramidal	1	Up

Table2. Lattice Parameters, X-Ray Density, Particle Size and Porosity SrLa_yFe_{12-x-y}Cr_xO₁₉

Samples	x	Molecular Weight (gm/mol)	2θ	Lattice Parameters		c/a (Å)	XRay Density (gm/cm ³)	Bulk Density (gm/cm ³)	Porosity (%)	Particle Size (Å)	Volume (Å ³)
				a (Å)	c (Å)						
S 1	0	1144.8091	32.42	5.826	23.527	4.038	5.496	2.777	49.4	7.237	691.65
S 2	2	1137.1111	32.47	5.819	23.481	4.035	5.462	2.619	52.7	36.19	691.27
S 3	4	1145.4137	32.52	5.812	23.435	4.030	5.549	2.428	54.5	12.065	688.68
S 4	6	1145.7157	10.95	5.805	23.356	4.035	5.546	2.399	56.3	34.908	685.98
S 5	8	1146.0179	32.37	5.794	22.206	3.832	5.894	2.377	59.4	7.617	645.66

Table 3 Electrical Conductivity Calculations for the samples SrLaCr_xFe_{11-x}O₁₉

Samples	X	Resistivity (ρ) at 300 K (Ω-cm)	Capacitance (F)	Dielectric Loss Factor(ε)	ΔE (eV)		Transition Temperature T _d (K)	Curie Temperature T _c (K)
					Para	Ferri		
S 1	0	1.23E+07	3.19E-11	4.28E-10	0.3026	0.6222	473	475
S 2	2	3.31E+05	2.46E-10	1.25E-08	0.5882	0.4483	513	518
S 3	4	1.22E+04	7.85E-09	1.02E-03	0.6588	0.3454	523	528
S 4	6	2.27E+05	1.26E-10	1.47E-10	0.732	0.3189	583	590
S 5	8	2.11E+07	3.19E-11	4.28E-10	1.0794	0.2641	598	604





Table 4 VSM Calculations for SrLaCr_xFe_{11-x}O₁₉

Sample s	x	Saturation Magnetization (emu/g)	RetentivityM r (emu/g)	Coercivity (Oe)	Bohr Magneton (μB)	Anisotropy Constant (K)	Mr/Ms
S 1	0	861.6	453.8	5375	176.62	2.32E+00	1.899
S 2	2	59.11	77.54	2250	14.16	2.38E-03	1.955
S 3	4	18.85	21.04	1250	0.42	3.23E-02	2.459
S 4	6	0.372	0.071	1000	0.39	1.86E-04	5.209
S 5	8	0.334	0.032	125	0.069	2.09E-05	10.61

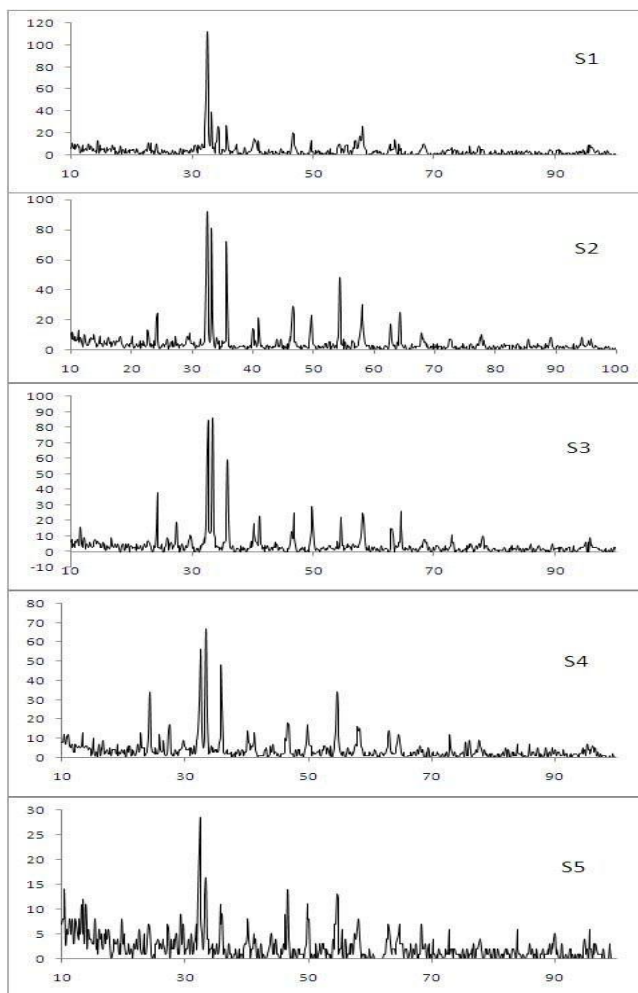


Figure 2. XRD pattern at room temperature of SrLa_yFe_{12-x-y}Cr_xO₁₉.

